Atmospheric
Measurement
Techniques
Open Access
Discussions

Improving satellite retrieved aerosol microphysical properties using GOCART data

S. Li[1,2], R. Kahn[3], M. Chin[3], M.J. Garay[4], L. Chen[1], and Y. Liu[2]

[1]State Key Laboratory of Remote Sensing Science, Jointly Sponsored by the Institute of Remote Sensing and Digital Earth of CAS and Beijing Normal University, Beijing, 100101, China
[2]Department of Environmental Health, Rollins School of Public Health, Emory University, Atlanta, GA 30322, USA
[3]Laboratory for Atmospheres, NASA Goddard Space Flight Center, Greenbelt, Maryland, USA
[4]Jet Propulsion Laboratory, California Institute of Technology, Pasadena, CA 91109, USA

Correspondence to: Y. Liu (yang.liu@emory.edu) and L. Chen (lfchen@irsa.ac.cn)

Title Page

Abstract | Introduction

Conclusions | References

Tables | Figures

|◄ | ►|

◄ | ►

Back | Close

Full Screen / Esc

Printer-friendly Version

Interactive Discussion

Abstract

The Multi-Angle Imaging Spectro-Radiometer (MISR) instrument on NASA's Terra satellite can provide more reliable Aerosol Optical Depth (AOD, τ) and more particle information, such as constraints on particle size (Angström exponent or ANG, α), particle shape, and single-scattering albedo (SSA, ω), than many other satellite instruments. However, MISR's ability to retrieve aerosol properties is weakened at low AOD levels. When aerosol-type information content is low, many candidate aerosol mixtures can match the observed radiances. We propose an algorithm to improve MISR aerosol retrievals by constraining MISR mixtures' ANG and absorbing AOD (AAOD) with Goddard Chemistry Aerosol Radiation and Transport (GOCART) model-simulated aerosol properties. To demonstrate this approach, we calculated MISR aerosol optical properties over the contiguous US from 2006 to 2009. Sensitivities associated with the thresholds of MISR-GOCART differences were analyzed according to the agreement between our results (AOD, ANG, and AAOD) and AErosol RObotic NETwork (AERONET) observations. Overall, our AOD has a good agreement with AERONET because the MISR AOD retrieval is not sensitive to different mixtures under many retrieval conditions. The correlation coefficient (r) between our ANG and AERONET improves to 0.45 from 0.29 for the MISR Version 22 standard product and 0.43 for GOCART when all data points are included. However, when only cases having AOD > 0.2, the MISR product itself has $r \sim 0.40$, and when only AOD > 0.2 and the best-fitting mixture are considered, $r \sim 0.49$. So as expected, the ANG improvement occurs primarily when the model constraint is applied in cases where the particle type information content of the MISR radiances is low. Regression analysis for AAOD shows that MISR Version 22 and GOCART misestimate AERONET by a ratio (mean retrieved AAOD to mean AERONET AAOD) of 0.5; our method improves this ratio to 0.74. Large discrepancies are found through an inter-comparison of the spatial-temporal patterns of MISR, GOCART, and our adjusted aerosol optical properties. We attribute these differences to (1) GOCART underestimations of AOD and ANG in polluted regions due to the emissions inventories

used, and not considering the fine particles such as nitrate, (2) a lack of certain aerosol mixtures in the Version 22 algorithm climatology, (3) a lack of sensitivity in the MISR radiances to particle type under some conditions, and (4) parameters and thresholds used in our method.

1   Introduction

Atmospheric aerosols affect global climate change directly by absorbing and reflecting solar radiation (Myhre, 2009) and indirectly by altering cloud microphysics and bio-geochemical cycles (Mahowald, 2011). Despite decades of research, the quantitative relationships among aerosols, clouds, and precipitation with the global climate system are still not well understood due to the inadequacy of existing tools and methodologies (Stevens and Feingold, 2009) and available measurements. Aerosol particles originate from a wide variety of natural and anthropogenic sources, and may contain chemically distinct species such as sulfates, nitrates, organic carbon (OC), black carbon (BC), sea salt, and mineral dust. The concentration and composition of these species are temporally and spatially highly variable. Ground-based observations, such as those provided by the AErosol RObotic NETwork (AERONET), are often used to constrain total-column aerosol optical properties, but these point measurements have very limited spatial coverage (Holben et al., 1998), and the derivation of particle properties other than the spectral optical depth or Angström exponent (ANG) requires many assumptions. During the past decade, researchers have explored the potential of using satellite-retrieved aerosol properties to fill in the gaps not covered by ground observations. The satellite products have advanced our understanding of the impact of aerosols on global climate change (Lohmann and Lesins, 2002), air quality (Liu et al., 2009b), particle type (Liu et al., 2007a; Kahn and Limbacher, 2012), and public health (van Donkelaar et al., 2010).

Uncertainties in satellite aerosol retrievals are usually attributed to cloud contamination, surface reflectance estimation, and the selection of aerosol optical models (Chu

et al., 2002). Among these factors, the aerosol models are usually derived from the analysis of ground-based observations, such as AERONET data or aircraft in situ measurements acquired during field campaigns. Omar et al. (2005) found that six aerosol models (composed of desert dust, biomass burning, background/rural, polluted continental, marine, and dirty pollution aerosol) represented the primary aerosol types in almost the entire AERONET dataset. With slight modifications, these aerosol types are used in the operational Cloud-Aerosol Lidar and Infrared Pathfinder Satellite Observation (CALIPSO) lidar aerosol classification algorithm (Omar et al., 2005). As the most popular aerosol product, NASA's Moderate Resolution Imaging Spectroradiometer (MODIS) assigns a set of global aerosol models in its Dark Target (DT) algorithm (Levy et al., 2007), based on spatial and temporal information derived from AERONET. Many researchers also use local observations to bridge the gaps created by global aerosol products. For example, Li et al. (2005a) derived seasonal aerosol mixing ratios with SSA around 0.91–0.94 to accommodate the higher aerosol absorption encountered in Hong Kong. Lee and Kim (2010) achieved better AOD correlations with AERONET than those assumed in the operational MODIS aerosol products when using aerosol models developed by statistically clustering the observational data from East Asia. However, AERONET network coverage is not dense enough to capture all the subtlety in aerosol type diversity on continental scales. To date, many studies have demonstrated that atmospheric Chemical Transport Models (CTM) can help constrain satellite aerosol retrievals. Drury et al. (2008, 2010) first coupled the simulated aerosol properties from a global 3-D chemical transport model (GEOS-Chem) to improve the MODIS DT algorithm. This method was extended by Wang et al. (2010) and Li et al. (2013), who looked specifically at dust and haze pollution in China and demonstrated better performance of customized retrievals than the MODIS standard product. Although the accuracy of most CTM simulations, like those from GEOS-Chem, depends heavily on the quality of meteorological inputs, atmospheric chemistry schemes, and emission inventories, CTM simulations have the advantage of providing information

on aerosol mass concentration, composition, and optical properties at regional–to–global scales with complete temporal and spatial coverage.

The MODIS instruments have proven valuable for retrieving AODs around the world, but the standard DT algorithm shows poor performance over bright surfaces and lacks the capability to retrieve additional aerosol optical properties, such as particle type. The analysis presented in this paper focuses on the Multi-angle Imaging SpectroRadiometer (MISR), which was launched into a sun-synchronous polar orbit in December 1999 aboard the NASA Earth Observing System (EOS) Terra satellite. With a unique design of nine individual cameras, MISR does not rely on an assumed relationship of surface reflectance between shortwave infrared and visible bands, as the MODIS DT algorithm does. Instead, it uses the presence of angular-spatial patterns within a 17.6 km retrieval region to derive an empirical orthogonal function (EOF) representation of the region-averaged, surface-leaving light reflection (Martonchik et al., 2009). The EOF algorithm can greatly reduce the impact of surface reflectance uncertainties (Diner et al., 2005). Global validation of MISR-retrieved AOD against AERONET observations showed that the operational (Version 22) MISR AOD product has a retrieved error that is the larger of ±0.05 or ±0.2τ (Kahn et al., 2010). The retrieval algorithm that generates this product defines 74 aerosol optical models (called "mixtures" in MISR terminology), which are combinations of up to three of eight individual aerosol components, each defined by a size distribution, shape, and complex index of refraction. The top-of-atmosphere (TOA) reflectances calculated based on these aerosol mixtures and stored in a look-up table are compared with the observed reflectance; then, a set of chi-square statistical tests is developed to determine which aerosol mixtures provide the best fits to the observations (Kahn et al., 1998; Liu et al., 2009a). Using this approach, the V22 MISR aerosol retrieval algorithm provides some particle type information, in addition to AOD, such as constraints on ANG and SSA, under favorable retrieval conditions.

However, the V22 MISR aerosol retrieval approach also has limitations. Although the mixtures included in the MISR algorithm were derived primarily from field measurements, selections among these mixtures are based on a set of chi-square statistical

Title Page

Abstract | Introduction

Conclusions | References

Tables | Figures

|◄ | ►|

◄ | ►

Back | Close

Full Screen / Esc

Printer-friendly Version

Interactive Discussion

tests that do not employ any prior spatial or temporal aerosol information (e.g., the prior information from AERONET that defines the aerosol optical properties used in the MODIS DT algorithm). If many different mixtures pass the retrieval acceptance criteria, this usually indicates that the aerosol-type information content of the observations is limited (Kahn et al., 2010) and the retrieved type might reflect more on the MISR algorithm aerosol climatology than the true aerosol properties (Liu et al., 2007a, b). Liu et al. (2007a) reported ∼ 20% uncertainty in MISR-retrieved aerosol microphysical properties when distinguishing light-absorbing and non-light-absorbing aerosols. The sensitivity of the V22 MISR retrieval algorithm to aerosol component information also diminishes when AOD is below 0.15 or 0.2 (Kahn et al., 1997, 2001). Moreover, the V22 MISR algorithm climatology lacks spherical absorbing particles of certain sizes, as well as mixtures containing both spherical, absorbing smoke analogs and non-spherical dust. For these reasons, the V22 MISR algorithm shows poor AOD performance for some biomass burning and urban regions (Kahn et al., 2007, 2010). ANG also tends to be overestimated in dusty regions, as the current set of eight aerosol components lacks medium particles with effective radii between 0.26 and 2.8 µm (Kahn et al., 2010).

Our work aims to improve retrievals of MISR aerosol optical properties by using CTM aerosol simulations as additional constraints on particle type where the MISR radiances lack such sensitivity. We used the GOCART model because it has been evaluated against sun photometer measurements and satellite observations around the world (Chin et al., 2009), and this global-scale model can provide a useful link between satellite and ground observations (Chin et al., 2002). For example, GOCART can provide MISR corresponded parameters such as AOD, ANG and AAOD, which can also be validated using AERONET observations. The rest of the paper is organized such that Sect. 2 describes the various datasets involved in this analysis and the methods used for constraining MISR mixtures by CTM simulations. Section 3 validates our method using four years of AERONET observations over the contiguous US. The sources of uncertainties and sensitivity analysis are also discussed in detail

in this section. Finally, major findings and potential future improvements to the current analysis are summarized in Sect. 4.

2   Data and method

2.1   MISR aerosol product

The MISR Level 2 aerosol data (Version 22), with a spatial resolution of 17.6 km, were downloaded from the NASA Langley Research Center Atmospheric Sciences Data Center (http://eosweb.larc.nasa.gov) for the contiguous US from 2006 through 2009. Total column AOD values used in this analysis are from MISR parameters "RegBestEstimateSpectralOptDepth" and "RegLowestResidSpectralOptDepth" (called "MISR Best Estimate" and "MISR Lowest Resid" hereinafter), which represent the mean AOD of all mixtures that pass the goodness-of-fit tests and the AOD of the mixture having the smallest chi-square, respectively (Martonchik et al., 1998). The corresponding parameters for ANG ("RegBestEstimateAngstromExponent" and "RegLowestResidAngstromExponent") and SSA ("RegBestEstimateSSA") were also extracted. The ANG reported in the MISR product is calculated from the slope of a linear least squares fit to the AODs retrieved at MISR's four wavelengths (446, 558, 672, and 866 nm). The AAOD ($\tau^{\text{absorbing}}$) at a given wavelength can be calculated by SSA and AOD according to Eq. (1):

$$\tau^{\text{absorbing}} = \tau \cdot (1 - \omega) \tag{1}$$

MISR's 74 mixtures are made up of one or more "pure" aerosol components corresponding to spherical non-absorbing aerosol (components 1, 2, 3, and 6, representing sulfate, sea salt, organic aerosol, etc., optical analogs), spherical, absorbing aerosol (components 8 and 14, representing black or brown carbon aerosol, etc.), and non-spherical dust analogs (components 19 and 21) (Kahn et al., 2010). A "mixture data" table in the MISR product (as shown in Fig. 1) lists each mixture's properties, such

Title Page

Abstract	Introduction
Conclusions	References
Tables	Figures

◄ | ►

◄ | ►

Back | Close

Full Screen / Esc

Printer-friendly Version

Interactive Discussion

as ANG (reported in "Angstrom exponent"), SSA (reported in "Mixture spectral single scattering albedo"), and the fractional contribution of component to the total AOD (reported in "Component fractional optical depth in reference band"). MISR also provides information on whether each mixture passed the goodness-of-fit tests (reported in "AerRetrSuccFlagPerMixture"), the number of successful mixtures (reported in "NumSuccAerMixture"), and the green-band (558 nm) AOD for each of the 74 mixtures used in the retrieval (reported in "OptDepthPerMixture"). Therefore, the aerosol optical properties can be calculated based on these mixtures and their related information.

2.2 GOCART aerosol simulations

The NASA GOCART model is driven by assimilated meteorological fields, which are generated in the Goddard Earth Observing System Data Assimilation System (GEOS DAS). Although the GOCART model has been validated around the world (Chin et al., 2009), our approach will also conduct a focused validation study for the same period and geographic region as the MISR retrievals. The GOCART 2-D simulations used in this analysis are at a 3 h temporal resolution and $1°$ latitude $\times$ $1.25°$ longitude horizontal resolution. Total column AOD (τ) at 550 nm is the sum of five tracer AODs, including sulfate, dust, OC, BC, and sea salt, as shown in Eq. (2):

$$\tau = \tau_{\text{sulfate}} + \tau_{\text{dust}} + \tau_{\text{OC}} + \tau_{\text{BC}} + \tau_{\text{sea-salt}} \tag{2}$$

GOCART saves 2-D AOD at 7 wavelengths (350, 450, 550, 650, 900, 1000, and 1500 nm). ANG is calculated from AODs at 450 nm and 900 nm using the Angstrom Equation ($\alpha = -\frac{\ln \frac{\tau_{450}}{\tau_{900}}}{\ln \frac{450}{900}}$). The model also provides the absorbing AOD at 7 wavelengths for each tracer; thus, the total absorbing AOD at 550 nm can be calculated by Eq. (3):

$$\tau^{\text{absorbing}} = \tau_{\text{dust}}^{\text{absorbing}} + \tau_{\text{OC}}^{\text{absorbing}} + \tau_{\text{BC}}^{\text{absorbing}} \tag{3}$$

The factors that affect GOCART AOD the most are the particle mass and the assumed aerosol optical properties. The uncertainties in the simulated aerosol mass are

attributed primarily to ground emissions and meteorological fields. Because sulfate and sea salt particles are non-absorbing at visible wavelengths, they are not included in Eq. (3).

As shown in Fig. 2, there are 690 GOCART grid cells over the contiguous US. To compare the satellite retrievals with model simulations, all MISR cloud-free 17.6 km pixels located in each $1° \times 1.25°$ GOCART grid cell were first averaged (called $MISR_{GOCART}$ hereinafter). Then, GOCART simulations at 12 p.m. local time, which roughly corresponds to the MISR overpass time ($\sim$ 10.30 a.m. local time), were sampled at the $MISR_{GOCART}$ swath. Figure 2 also adds the National Land Cover Database (NLCD) 2006 land cover layer, which is partly linked to the ground emission conditions (Wang et al., 2012). Due to the large differences of land cover, climate, and emissions, we divided the contiguous US into eastern and western regions along the 100° W longitude line.

2.3 AERONET Level 2 data

During our study period, there were 32 AERONET sites with Level 2 (quality assured) spectral AOD data (accessed at http://aeronet.gsfc.nasa.gov). As shown in Fig. 2, 14 of these AERONET sites (red circles) are in the Eastern US, many of which are located along the Atlantic coast. There are 18 Western AERONET sites, many of which are in crop- or forest-covered regions, according to the NLCD 2006 land cover data. AERONET AOD values are typically recorded by sun photometers every 15 min in seven spectral bands (340, 380, 440, 500, 670, 870, and 1020 nm). AERONET AOD values at 440 nm and 870 nm were used to calculate ANG using the Angstrom Equation above, which was then used to interpolate the AOD to 550 nm to compare with the GOCART and MISR AOD data (558 nm). AERONET observations were averaged over a two-hour window surrounding the 10.30 a.m. local time satellite overpass to match the satellite overpass time. AERONET AAOD is only considered of high quality when the AOD at 440 nm is greater than 0.4 and the solar zenith angle is larger than 50°

(Dubovik et al., 2000, 2002). Figure 2 shows the 18 AERONET sites (blue circles) that reported the absorbing AOD and SSA during this period.

2.4 Constraining MISR mixtures with GOCART data

As mentioned above, greater uncertainty in MISR-retrieved aerosol microphysical prop-
erties is indicated when many mixtures satisfy the retrieval criteria (Liu et al., 2007a, b). The post-processing technique proposed in this analysis aims at narrowing the se-
lection of mixtures by introducing GOCART aerosol simulation results. Our approach does not require rebuilding the MISR look-up table or rewriting the EOF code. Instead, we use model-simulated "ANG" and "AAOD" to constrain the MISR mixture selection reported in the V22 operational product. ANG and AAOD are obtained from GOCART simulations and AERONET observations. This additional information provides some constraints on aerosol size distribution and composition. We use AAOD rather than SSA (ϖ) since AAOD is less sensitive to cloud contamination and aerosol hygroscopic growth (Kaufman et al., 1997; Hu et al., 2009).

In practice, we constrain MISR's aerosol mixture selections with GOCART aerosol simulation results by calculating the differences of ANG and AAOD between MISR and GOCART:

$$\text{Diff}_{\text{ANG}} = |\alpha_{\text{MISR}} - \alpha_{\text{GOCART}}| \leq \varepsilon_{\text{ANG}} \tag{4}$$

$$\text{Diff}_{\text{AAOD}} = \left|\text{Fraction}_{\text{MISR\_AAOD}} - \text{Fraction}_{\text{GOCART\_AAOD}}\right| \leq \varepsilon_{\text{AAOD}} \tag{5}$$

where ε_{ANG} and $\varepsilon_{\text{AAOD}}$ represent the corresponding thresholds for ANG and AAOD differences, evaluated between 440 and 870 nm, and at 558 nm, respectively. $\text{Fraction}_{\text{MISR\_AAOD}}$ is the fractional contribution of AAOD to the total AOD for a specific mixture at 558 nm. The corresponding $\text{Fraction}_{\text{GOCART\_AAOD}}$ is calculated as $\frac{\tau_{\text{GOCART}}^{\text{absorbing}}}{\tau_{\text{GOCART}}}$. This process emphasizes the absorbing aerosol contribution and reduces the impact of differences in the absolute AAOD values due to model-satellite discrepancies. Because a fixed threshold of ε_{ANG} or $\varepsilon_{\text{AAOD}}$ often leaves no mixtures that meet the acceptance

criteria, we adopted dynamic thresholds in Eqs. (4) and (5) to retain a certain percentage of mixtures (e.g., a% means that we keep "a% × No. of successful mixtures" mixtures). Specifically, we first sorted the absolute differences calculated by Eqs. (4) and (5) in order from small to large values, then selected those at the top a%. The minimum (0 %) and maximum (100 %) values represent none and all MISR successful mixtures passing our thresholds, respectively. New aerosol optical properties can be calculated after the constrained subset of MISR-retrieved mixtures is determined. We expect this approach to help primarily in situations where aerosol type information is lacking in the MISR radiances, though not when the key aerosol optical analogs are altogether missing in the V22 algorithm climatology. The errors in our method are mainly due to the uncertainties in the GOCART simulations, limitations in the V22 MISR mixture distribution, and thresholds of $\varepsilon_{\mathrm{ANG}}$ or $\varepsilon_{\mathrm{AAOD}}$, which are discussed in turn in later sections.

3 Results and discussion

3.1 Validation of MISR and GOCART products with AERONET observations

We first validated the corresponding MISR and GOCART standard products against AERONET observations. During the period 2006 through 2009, there were 1492 MISR-AERONET matched data records for AOD and ANG over the 32 AERONET sites. Figure 3 shows that both "MISR Best Estimate" and "MISR Lowest Resid" AOD retrievals are strongly correlated with AERONET data ("MISR Best Estimate": $y = 0.8x + 0.05$, r: 0.79; "MISR Lowest Resid": $y = 0.8x + 0.05$, r: 0.78). The agreement between "MISR Best Estimate" and "MISR Lowest Resid" was also reported in previous studies (Liu et al., 2004). Our validation effort confirms that MISR-retrieved AOD is fairly robust, even when the retrieved particle properties are not well constrained (Kahn et al., 2001, 2010). Compared to the MISR retrievals, GOCART yields a smaller value for the slope and correlation coefficient against AERONET AOD ($y = 0.27x + 0.06$, r: 0.5). Many

factors may contribute to these results. The model AOD calculation is based on parti-
cle mass and assumed aerosol optical parameters (Martin et al., 2003). First, uncer-
tainties in the simulated aerosol mass may be attributed to the emissions inventories
used, wet and dry deposition parameterizations, chemical evolution mechanisms, and
meteorological fields (e.g. relative humility). Second, optical parameters such as mass
extinction efficiency and effective radius assumed by the model may be wrong if inap-
propriate or incorrect aerosol hygroscopic factors, complex refractive indices, and size
distributions were used. For example, GOCART does not consider any internal mixture,
ultra-fine particles, and the absorption and hygroscopic growth of organic aerosols.
Most importantly, high AOD values (e.g., AOD > 0.5) typically occur only over source
regions, which are too small to be resolved by the model. Thus, the coarse resolution of
GOCART simulations ($1° \times 1.25°$) covering primarily low-AOD regions results in lower
mean AOD values than those produced by AERONET point observations (Cheng et al.,
2012), and the GOCART-AERONET comparison has limited value as a quantitative
AOD validation. Nevertheless, the GOCART model reproduces the correct seasonal
variations at most sites, especially in places where biomass burning or dust aerosol
dominates (Chin et al., 2002). Figure 3.1c also indicates that both the mean value of
GOCART AOD (Mean_O:0.09) and the mean of the absolute difference (Diff: 0.05) are
comparable with those of AERONET (Mean_A:0.1) and MISR (Diff: 0.05).

Linear regression of the "MISR Best Estimate" ANG against the AERONET obser-
vations, for all data regardless of AOD, yields an r of 0.29, a slope of 0.28, an intercept
of 0.91, and a Diff of 0.41 (Fig. 3.2a). Although the values of ANG among 74 MISR
mixtures have a wide range (from 3.8 to −0.2, as shown in Fig. 1), if many different
mixtures meet the MISR algorithm acceptance criteria, ANG calculated from the aver-
age of AOD values obtained in each MISR spectral channel tends towards the mean
value of unity (Kahn et al., 2009). Moreover, when mid-visible AODs are below about
0.15 or 0.2, which occurs commonly in the US, there is less particle property informa-
tion in the MISR radiances, resulting in poor ANG retrievals (Kahn et al., 2009). This is
borne out by the red points in Fig. 3.2a, which are only for AOD > 0.2. For these points,

the correlation coefficient improves from 0.29 to 0.40, and the Diff reduces to 0.36. Similarly, Fig. 3.2b shows the relationships between "MISR Lowest Resid" and AERONET ANG in black; and "MISR Lowest Resid" and AERONET ANG only for AOD > 0.2 in red. Again, the correlation coefficient improves significantly from 0.23 for the entire dataset to 0.49 for AOD > 0.2, and the Diff reduces to 0.35.

Compared to the MISR data, GOCART-simulated ANG shows comparable agreement with AERONET when the AOD is restricted to be greater than 0.2, and shows better performance (r: 0.43, Diff: 0.33) than MISR when all data are included, mainly because low-AOD does not reduce the aerosol type information in the model. However, the largest limitation of GOCART is due to not assuming the fine particles such as nitrate, which results in ANG > 2 cannot be simulated in GOCART. Even so, aerosol type constraints from the model should be particularly valuable for the prevailing number of situations in the US that have total AOD less than 0.2, as the GOCART model is adjusted to match observations as much as possible and, through the use of emissions inventories, is better able to capture the overall spatial and temporal features of the validation data sets used (Russell et al., 2010; Reid et al., 1999). Because there are just 156 records in contiguous US when AOD is greater than 0.2 (10.5 % of 1492 total cases), these results demonstrate the usefulness of external constraints from a CTM model, particularly when the particle property information content of the MISR radiances is limited.

Given that both the AOD and solar zenith angle conditions are required for such retrievals, there are far fewer AERONET sky-scan AAOD retrievals compared with direct-sun AOD measurements, and many more assumptions are required to derive aerosol absorption. In our analysis, we found only 107 matched MISR-AERONET AAOD data records, compared with 1492 AOD matches, making our results less statistically robust. "MISR Best Estimate" AAOD at 558 nm, with a mean value of 0.009, is much lower than the AERONET AAOD (0.018), and the Diff is as high as 0.013. We calculated the ratio of mean retrieved AAOD to mean AERONET AAOD (γ: 0.5) and the regression slope (0.36) with no intercept (zero) to show its underestimation, and no correlation coefficient

is shown due to the poor agreement. "MISR Lowest Resid" AAOD shows similar under-estimation with a γ of 0.56, a slope of 0.39, and a Diff of 0.013. The underestimation of the V22 MISR AAOD is expected; it occurs because spherical absorbing aerosol optical analogs are lacking in the V22 MISR aerosol climatology (Kahn et al., 2010), so SSA generally tends to be too high in places where absorbing aerosol occurs, and MISR AAOD would be too low. In addition to the lack of certain absorbing spherical particle sizes, another contributing factor is that the aerosol loading in the contiguous US is too low to provide more AAOD or SSA information in the MISR radiances. We re-analyzed the AAOD comparison for AOD > 0.5 (red points in Fig. 3.3a and b), and both "MISR Best Estimate" and "MISR Lowest Resid" AAOD ratios (γ) improved to 0.61 and 0.65, respectively. The GOCART model also underestimated the AAOD with a mean value of 0.009, giving a low γ of 0.5 and a slope of 0.34. Similar underestimation for GOCART AAOD simulations in the US was also found in a previous study (Chin et al., 2009).

3.2 Sensitivity analysis and validation of our algorithm

Our validation suggested that the "MISR Best Estimate" and "MISR Lowest Resid" parameters could be used interchangeably for AOD, whereas both parameters show generally poor performance for ANG and AAOD, due in part to particle property limitations in the V22 MISR standard algorithm, and in part to low aerosol loading conditions, that occur frequently over the US. The purpose of this analysis is to test the use of aerosol mixtures from GOCART simulations; therefore, "MISR Best Estimate," which contains more mixtures, was chosen to be the representative MISR aerosol parameter. As mentioned in Sect. 2.4, the uncertainty in our algorithm can be attributed to the thresholds ε_{ANG} and ε_{AAOD} in Eqs. (4) and (5), in addition to the quality of the model simulations. The goal of the sensitivity analysis in this section is to select the optimum thresholds to achieve better agreement between our results (AOD, ANG, and AAOD) and those of AERONET. We used the correlation coefficients of AOD (r_{AOD}) and ANG (r_{ANG}) between MISR and AERONET and the ratio of mean MISR AAOD to mean AERONET

AAOD (γ_{AAOD}) to form the assessment index for our method. Figure 4 shows the distributions of r_{AOD}, r_{ANG}, and γ_{AAOD}, with ε_{ANG} and ε_{AAOD} varying from 0 % to 100 %. As described in Sect. 2.4, a % of ε_{ANG} and ε_{AAOD} means using MISR-GOCART ANG and AAOD differences to keep "a% × No. of successful mixtures" mixtures, respectively. When both ε_{ANG} and ε_{AAOD} are 100 %, our r_{AOD}, r_{ANG}, and γ_{AAOD} are equal to the original corresponding MISR correlation coefficients and ratios in Fig. 3.

When ε_{ANG} or ε_{AAOD} is lower than 30 %, our r_{AOD} increases with the number of successful mixtures. When both ε_{ANG} and ε_{AAOD} are larger than 30 % (inside the red region of Fig. 4a), r_{AOD} is stable at a relatively high value (> 0.75), almost equal to the original $r_{MISR-AOD}$ (0.79) in Fig. 3a. Our findings here indicate that MISR AOD retrieved by the operational algorithm is at least as good- and is often better-than the corresponding GOCART values and is probably not sensitive to aerosol mixtures, especially for mid-visible AOD below about 0.15 or 0.2. This is also discussed by Kahn et al. (2001, 2010). Referring back to Fig. 3.1a and b, the latter result is supported by the small differences between "MISR Best Estimate" and "MISR Lowest Resid" AOD. In general, MISR AOD retrievals contain unique information that the transport model is unlikely able to improve upon, except to the extent that aerosol type affects the result, which occurs preferentially at higher AOD.

Our r_{ANG} is negatively correlated with ε_{ANG}, as might be expected (a tighter ANG agreement threshold produces better correlation), but is generally positively correlated with ε_{AAOD}. When ε_{AAOD} is low, r_{ANG} usually increases with the ε_{AAOD} value, indicating better ANG results when very tight agreement with transport model absorption is not required; this is probably related to the MISR V22 climatology containing only a single size of spherical absorbing particles (Kahn et al., 2010). When ε_{AAOD} is larger than 40 %, r_{ANG} depends strongly on ε_{ANG} and is mostly independent of ε_{AAOD}, reflecting greater sensitivity to particle size than absorption (Kahn et al., 1998). Our analysis indicates that setting a relatively stringent (low) GOCART ANG threshold can significantly improve the correlation between our ANG and AERONET. As shown in the red region

Improving satellite retrieved aerosol microphysical properties using GOCART data

S. Li et al.

Title Page

Abstract | Introduction

Conclusions | References

Tables | Figures

|◄ | ►|

◄ | ►

Back | Close

Full Screen / Esc

Printer-friendly Version

Interactive Discussion

of Fig. 4b, r_{ANG} approaches 0.43, which is much higher than the original $r_{MISR-ANG}$ (0.29) in Fig. 3.2a.

The relationship between our γ_{AAOD} and the values of ε_{AAOD} and ε_{ANG} is complex. When ε_{AAOD} is higher than 60 %, our γ_{AAOD} is negatively correlated with ε_{ANG}. How-
ever, when $\varepsilon_{ANG} < 60$ %, ε_{ANG} does not have a significant effect on γ_{AAOD}, and γ_{AAOD} trends to increase with the ε_{AAOD} value. That is, once the particle size is adequately constrained by the model, our method uses any remaining particle absorption flexibility in the MISR V22 algorithm's aerosol climatology to further refine the choice of aerosol type. As shown in the red region of Fig. 4c, when ε_{AAOD} is roughly lower than 60 % and
ε_{ANG} is higher than 20 %, γ_{AAOD} could be in the range of 0.7 ∼ 0.82, which is much higher than the original $\gamma_{MISR-AAOD}$ (0.5) in Fig. 3.3a.

A set of appropriate thresholds should improve r_{AOD} and r_{ANG}, while keeping γ_{AAOD} close to 1.0. By checking the overlapping parts of the red regions among Fig. 4a–c, we set ε_{ANG} and ε_{AAOD} equal to 30 and 50 % (the black crosses in Fig. 4), respec-
tively. In this case, we compared our AOD, ANG, and AAOD results against AERONET observations as in the MISR and GOCART validation effort. Meanwhile, our summary statistics stratified by geographic location and season are presented in Table 1. For AOD, our mean value (0.13) is same as that of MISR and is higher than the AERONET observation (0.1) because the value in the West is overestimated (AERONET: 0.09,
our work: 0.14). AOD varies greatly by season for both AERONET and our results; AODs in the summer (AERONET: 0.13, our work: 0.16) were twice as high as in the winter (AERONET: 0.06, our work: 0.08). Overall, our AOD agrees well with AERONET ($y = 0.79x + 0.04$; $r = 0.79$; Diff = 0.04) and is similar to that of the MISR operational data shown in Fig. 3, but there are significant geographical and seasonal differences.
Better correlation is seen in the East (0.87), summer (0.78), and fall (0.88). For ANG, our mean value (1.21) is comparable with that of the AERONET observations (1.27), with a slight underestimation in all seasons except winter. Both AERONET and our results yield low ANG values in spring (AERONET: 1.06, our work: 0.97), the West (AERONET: 1.19, our work: 1.15); and at high AOD values in fall (AERONET: 1.4,

our work: 1.36) and the East (AERONET: 1.39, our work: 1.31). Overall, the ANG Diff (0.32), slope (0.29), and correlation coefficient (0.45) are better than those of the original MISR and GOCART data in Fig. 3.2. The best agreement (Diff: 0.28, $y = 0.3x + 0.63$, r: 0.5) is found in spring. For AAOD, our method improves the values of mean AAOD (0.013) and ratio (0.74), compared to those in MISR in Fig. 3.3a, especially where MISR information content is lacking. However, the mean difference is still significant (0.011), and the slope is slightly low (0.55). It is mainly because the threshold used in our method is set according to the ratio over the entire US, more analysis and adjustments should be conducted in our method based on regions, seasons, and other parameters. For example, the agreement in the West ($y = 0.95x$, $\gamma = 0.95$) and in the fall ($y = 0.68x$, $\gamma = 0.89$) is much better than in the East ($y = 0.44x$, $\gamma = 0.66$) and in the spring ($y = 0.23x$, $\gamma = 0.34$). We also conducted the comparison between two groups (AOD and ANG is grouped by AOD ≤ 0.2 and AOD > 0.2; AAOD is grouped by AOD ≤ 0.5 and AOD > 0.5). For AOD, we get the similar agreement for total AOD and grouped AOD (and the original MISR product, i.e., the method has little effect on the AOD results). For ANG and AAOD, the correlations at lower AOD conditions (ANG r: our = 0.41 vs. MISR = 0.27; AAOD γ: our = 0.73 vs. MISR = 0.46) are improved more significantly than those at higher AOD conditions (ANG r: our = 0.5 vs. MISR = 0.4; AAOD γ: our = 0.75 vs. MISR = 0.61). Therefore, our model constraints are particularly useful when the aerosol type information content of the MISR data is low.

3.3 Spatial-temporal patterns of MISR, GOCART, and our aerosol optical properties

We compared the seasonal distribution of AOD, ANG, and AAOD (Figs. 5–7) from MISR, GOCART, and our results over the contiguous US. We also present the summary statistics for the mean value of entire dataset, as well as the data stratified by season and location, in Table 2.

As shown in Fig. 5 and Table 2, our AOD has a similar spatial distribution and value range with MISR. Geographically, both MISR (0.16) and our results (0.15) show that

the East generally has higher AOD values than the West (0.13). Higher AOD values are found over relatively populated and polluted regions, such as the East Coast and the Great Lakes states. In the West, MISR and our results are also comparable with the AERONET AOD distribution. Our findings here are very similar to the previous study by Chatterjee et al. (2010). With the unique multi-angle design and EOF algorithm, MISR can better reduce the bias caused by surface reflectance (Diner et al., 2005) than other sensors, such as MODIS, and thus can retrieve more reliable AODs over bright surfaces, including deserts (Martonchik et al., 2004). Seasonally, Table 1 indicates both the MISR and our results yield the highest AOD for the study region in summer (0.18) and spring (0.17), followed by fall (MISR: 0.1, our work: 0.097) and winter (MISR: 0.083, our work: 0.082). Compared to MISR retrievals, GOCART generally has the similar spatial-temporal distribution. However, GOCART does not capture the high AOD values at more polluted sites, such as CCNY and Fresno in spring and summer, due to coarse sampling as explained earlier, but when the aerosol loading is low (e.g., in the West, Fall and Winter), GOCART can simulate AOD reliably close to those given by AERONET.

Figure 6 and Table 2 show the spatial-temporal patterns and the mean value of our ANG (1.22) is between MISR (1.24) and GOCART (1.19), as expected. Geographically, all three datasets show ANG values in the East (MISR: 1.34, GOCART: 1.24, our result: 1.28) are significantly higher than those in the West (MISR: 1.16, GOCART: 1.14, our result: 1.15). Seasonally, all three datasets indicate the minimum ANG values are found in spring (MISR: 1.15, GOCART: 0.94, our work: 1). The low values found in the West and spring can probably be attributed to dust transport. Yu et al. (2012) found approximately 140 Tg of fine dust was exported from Asia in the spring of 2005. With this trans-Pacific transport, 56 Tg of dust reached the West Coast of North America, although these estimates are largely uncertain. The contribution of Asian dust becomes weaker in the summer and fall, and decreases to 30–50 % of the springtime maximum over the Eastern US (Fairlie et al., 2007), though there are also local dust sources in the western US. However, MISR ANG shows large uncertainties when dust particles are abundant, due to the limited non-spherical dust optical analogs in the Version 22

climatology. For example, Kalashnikova et al. (2005) found that lack of very absorbing, plate-like dust particles in MISR retrieval algorithm can lead to AOD underestimation, and may thus introduce bias in ANG calculations. In the MISR research algorithm, arbitrarily large numbers of mixtures can be included, each of which can contain up to four individual aerosol components (Kahn et al., 2001). Our findings here support the idea that MISR retrieval would benefit from having more dust particle types and constraints from CTM simulations. Compared to MISR and AERONET data, GOCART ANG values in the East, especially for some Northeastern sites (e.g. GSFC), are significantly lower. Referring back to Fig. 3.2c, this underestimation may also contribute to those very low GOCART ANG values due to not considering the ultra-fine particles. Overall, the spatial-temporal distribution of our ANG is more similar to the GOCART distribution than MISR in the West in spring and summer, but is more similar to the MISR distribution than GOCART in the East of fall and winter.

Figure 7 and Table 2 show large AAOD distribution differences among the three datasets. The mean MISR AAOD (0.0035) in the contiguous US during 2006 to 2009 is much lower than the GOCART (0.0059) and our adjusted AAOD (0.0059). When we limited our data to those with column MISR AOD values greater than or equal to 0.2, which accounted for about 19 % of the raw data, the mean MISR AAOD increases to 0.0095. Like the validation in Sect. 3.1 and earlier work, it indicates more AAOD information can be inferred from the MISR radiances when AOD is high. GOCART shows smooth regional change in the contiguous US (mean AAOD around 0.006 for both the East and the West), except high AAOD values in the Southwest and Northeast, and the values in spring (0.0081) and summer (0.006) are higher than those of fall (0.0048) and winter (0.0039). Geographically, our AAOD distribution shows high-absorbing aerosol regions (e.g. the North and the Southeast) are similar to those in MISR, but the values are closer to those given by AERONET than MISR. Figure 7 indicates that there is a positive relationship between our high AAOD and the NLCD forest and shrubs land cover type (Fig. 2), where wildfires or prescribed burns can release more absorbing particles, such as BC and OC (Zhang and Kondragunta, 2008). The anthropogenic and

wildfire effluences from Western North America are mostly transported north and east, eventually merging with Eastern US pollution outflow to the Atlantic (Li et al., 2005b). The presence of elevated aerosol layers from biomass burning outflow across the Gulf of Mexico also has a large impact on the Southeast (Wang et al., 2009). Seasonally,

5 the relatively high values in our adjusted AAOD may be caused by dust transport in spring (0.007) and fire emissions in summer (0.0071) (Ichoku et al., 2008). As mentioned in Sect. 2.4, our AAOD depends not only on the MISR AOD values, but also on the fraction of GOCART AAOD and the successful MISR mixture distributions. Therefore, making quantitative improvements to the satellite component aerosol retrieval is

10 difficult. First, there are large uncertainties in GOCART data quality and MISR's ability to distinguish light-absorbing and non-absorbing aerosols (Kahn et al., 2001; Liu et al., 2007a). As mentioned before, if fewer absorbing mixtures pass the MISR EOF algorithm and/or an inappropriate GOCART AAOD fraction is used in our method, it would likely cause lower absorbing aerosol levels. Second, the value of SSA pre-defined in

15 the V22 MISR mixtures is too high for the contiguous US, making the AAOD is too low. As demonstrated with the MISR research algorithm by Kahn and Limbacher (2012) and Patadia et al. (2013), the current MISR V22 algorithm misses absorbing particles (the only spherical, absorbing particles all have 0.12 micron effective radius) and, in part, to low information content, especially at low AOD. To bridge the gaps, new aerosol optical

20 models need to be added to the Standard algorithm climatology (Kahn et al., 2010).

4   Conclusions

We have developed a new method to infer aerosol optical properties over land from the MISR standard aerosol product, in conjunction with GOCART simulations, and we applied this method to the contiguous US from 2006 to 2009. In this study, we first

25 processed a set of MISR successful mixtures, which contain AOD, ANG, SSA, and aerosol component information. We then obtained the corresponding aerosol optical properties from GOCART simulations to select subsets of those mixtures. The errors

in our method are mainly due to uncertainties in the GOCART and MISR measures of ANG and AAOD, and the differences between them. Sensitivity analysis shows setting the ANG and AAOD thresholds at almost 30 and 50 %, respectively, can achieve better agreement between our results (mainly ANG and AAOD) and those of AERONET for the entire US than with the original MISR data. Finally, new aerosol optical properties were calculated from the adjusted mixtures.

For comparison, we validated the MISR products and GOCART simulations of AOD, ANG, and AAOD by using coincident AERONET measurements, and estimated the seasonal distributions of these quantities over the contiguous US from 2006 to 2009. For AOD, a linear regression analysis using "MISR Best Estimate" and "MISR Lowest Resid" as the responses yields slopes of 0.8 and correlation coefficients up to 0.79. GOCART is unable to capture the aerosol variability at high AOD values, but the mean value and Diff are comparable to AERONET and MISR. Sensitivity analysis indicates the AOD values among different MISR mixtures are consistent. Thus, both the validation of our AOD and the mean values of seasonal distribution are very similar to the MISR operational product. Overall, the MISR EOF algorithm has the strong capability to retrieve AOD, even over the Western US, and it is very difficult to improve the AOD accuracy by only recombining the MISR mixtures. For ANG, both "MISR Best Estimate" and "MISR Lowest Resid" show a weak correlation with AERONET, except when the AOD is greater than about 0.2, as expected. However, GOCART can simulate ANG based on assumed size distributions, which is closer to AERONET values than retrieved by the V22 MISR algorithm. Sensitivity analysis indicates that using a stringent ANG threshold (30 %) can significantly improve correlation coefficient between our ANG and AERONET to 0.45. The best agreement (Diff: 0.28, r: 0.5) is found in spring, probably because GOCART provides good dust simulations. The spatial and temporal distribution of our ANG is more similar to the GOCART or MISR distribution when either performs well. All three datasets show the West and the spring have lower ANG values, due to the impact of dust. For AAOD, the values of "MISR Best Estimate", "MISR Lowest Resid" and GOCART are much lower than AERONET AAOD, with a ratio of

0.5, 0.56 and 0.5, respectively. Nevertheless, our method shows the model constraints can help improve the underestimated MISR AAOD. Sensitivity analysis indicates setting an AAOD threshold of 50 % can bring the ratio between our AAOD and AERONET to 0.74. Thus, our national mean AAOD value increases to 0.0059, compared to the value produced by MISR V22 (0.0035).

This study follows the previous works by (Drury et al., 2008; Wang et al., 2010; Li et al., 2013), who improved MODIS AOD under various conditions using the new GEOS-Chem aerosol model simulations. The current work in this field focuses on the limitations that are unresolved in this approach. We can address these issues by building more aerosol components and mixtures and introducing them into MISR retrieval (Kahn et al., 2010). This process will also require building new aerosol look-up tables and rerunning the EOF algorithm. Second, other CTMs like GEOS-Chem can be used to constrain MISR mixtures, especially when the information is lacking in the MISR radiances themselves, such as at low AOD. More sensitivity analyses should be conducted based on other aerosol parameters and assessment criteria. Finally, we plan to carry out this study in other regions, such as in developing countries with heavy anthropogenic (or absorbing) aerosols.

References

Chatterjee, A., Michalak, A. M., Kahn, R. A., Paradise, S. R., Braverman, A. J., and Miller, C. E.: A geostatistical data fusion technique for merging remote sensing and ground-based observations of aerosol optical thickness, J. Geophys. Res.-Atmos., 115, D20207, doi:10.1029/2009jd013765, 2010.

Cheng, T., Chen, H., Gu, X., Yu, T., Guo, J., and Guo, H.: The inter-comparison of MODIS, MISR and GOCART aerosol products against AERONET data over China, J. Quant. Spectrosc. Ra., 113, 2135–2145, doi:10.1016/j.jqsrt.2012.06.016, 2012.

Chin, M., Ginoux, P., Kinne, S., Torres, O., Holben, B. N., Duncan, B. N., Martin, R. V., Logan, J. A., Higurashi, A., and Nakajima, T.: Tropospheric aerosol optical thickness from the GOCART model and comparisons with satellite and Sun photometer measurements, J. Atmos. Sci., 59, 461–483, doi:10.1175/1520-0469(2002)059<0461:taotft>2.0.co;2, 2002.

Chu, D. A., Kaufman, Y. J., Ichoku, C., Remer, L. A., Tanre, D., and Holben, B. N.: Validation of MODIS aerosol optical depth retrieval over land, Geophys. Res. Lett., 29, MOD2.1–MOD2.4, doi:10.1029/2001gl013205, 2002.

Diner, D. J., Martonchik, J. V., Kahn, R. A., Pinty, B., Gobron, N., Nelson, D. L., and Holben, B. N.: Using angular and spectral shape similarity constraints to improve MISR aerosol and surface retrievals over land, Remote Sens. Environ., 94, 155–171, 2005.

Drury, E., Jacob, D. J., Wang, J., Spurr, R. J. D., and Chance, K.: Improved algorithm for MODIS satellite retrievals of aerosol optical depths over western North America, J. Geophys. Res.-Atmos., 113, D16204, doi:10.1029/2007jd009573, 2008.

Drury, E., Jacob, D. J., Spurr, R. J. D., Wang, J., Shinozuka, Y., Anderson, B. E., Clarke, A. D., Dibb, J., McNaughton, C., and Weber, R.: Synthesis of satellite (MODIS), aircraft (ICARTT), and surface (IMPROVE, EPA-AQS, AERONET) aerosol observations over eastern North America to improve MODIS aerosol retrievals and constrain surface aerosol concentrations and sources, J. Geophys. Res.-Atmos., 115, D14204, doi:10.1029/2009jd012629, 2010.

Dubovik, O., Smirnov, A., Holben, B. N., King, M. D., Kaufman, Y. J., Eck, T. F., and Slutsker, I.: Accuracy assessments of aerosol optical properties retrieved from Aerosol Robotic Network (AERONET) Sun and sky radiance measurements, J. Geophys. Res.-Atmos., 105, 9791–9806, doi:10.1029/2000jd900040, 2000.

Dubovik, O., Holben, B., Eck, T. F., Smirnov, A., Kaufman, Y. J., King, M. D., Tanre, D., and Slutsker, I.: Variability of absorption and optical properties of key aerosol types

Title Page

Abstract | Introduction

Conclusions | References

Tables | Figures

|◄ | ►|

◄ | ►

Back | Close

Full Screen / Esc

Printer-friendly Version

Interactive Discussion

observed in worldwide locations, J. Atmos. Sci., 59, 590–608, doi:10.1175/1520-0469(2002)059<0590:voaaop>2.0.co;2, 2002.

Fairlie, T. D., Jacob, D. J., and Park, R. J.: The impact of transpacific transport of mineral dust in the United States, Atmos. Environ., 41, 1251–1266, doi:10.1016/j.atmosenv.2006.09.048, 2007.

Holben, B. N., Eck, T. F., Slutsker, I., Tanre, D., Buis, J. P., Setzer, A., Vermote, E., Reagan, J. A., Kaufman, Y. J., Nakajima, T., Lavenu, F., Jankowiak, I., and Smirnov, A.: AERONET – a federated instrument network and data archive for aerosol characterization, Remote Sens. Environ., 66, 1–16, doi:10.1016/s0034-4257(98)00031-5, 1998.

Hu, R. M., Sokhi, R. S., and Fisher, B. E. A.: New algorithms and their application for satellite remote sensing of surface $PM_{2.5}$ and aerosol absorption, J. Aerosol. Sci., 40, 394–402, doi:10.1016/j.jaerosci.2009.01.005, 2009.

Ichoku, C., Giglio, L., Wooster, M. J., and Remer, L. A.: Global characterization of biomass-burning patterns using satellite measurements of fire radiative energy, Remote Sens. Environ., 112, 2950–2962, doi:10.1016/j.rse.2008.02.009, 2008.

Kahn, R. A. and Limbacher, J.: Eyjafjallajökull volcano plume particle-type characterization from space-based multi-angle imaging, Atmos. Chem. Phys., 12, 9459–9477, doi:10.5194/acp-12-9459-2012, 2012.

Kahn, R., West, R., McDonald, D., Rheingans, B., and Mishchenko, M. I.: Sensitivity of multiangle remote sensing observations to aerosol sphericity, J. Geophys. Res.-Atmos., 102, 16861–16870, doi:10.1029/96jd01934, 1997.

Kahn, R., Banerjee, P., McDonald, D., and Diner, D. J.: Sensitivity of multiangle imaging to aerosol optical depth and to pure-particle size distribution and composition over ocean, J. Geophys. Res.-Atmos., 103, 32195–32213, doi:10.1029/98jd01752, 1998.

Kahn, R., Banerjee, P., and McDonald, D.: Sensitivity of multiangle imaging to natural mixtures of aerosols over ocean, J. Geophys. Res.-Atmos., 106, 18219–18238, doi:10.1029/2000jd900497, 2001.

Kahn, R., Garay, M. J., Nelson, D. L., Yau, K. K., Bull, M. A., Gaitley, B. J., Martonchik, J. V., and Levy, R. C.: Satellite-derived aerosol optical depth over dark water from MISR and MODIS: comparisons with AERONET and implications for climatological studies, J. Geophys. Res.-Atmos., 112, D18205, doi:10.1029/2006jd008175, 2007.

Kahn, R., Nelson, D., Garay, M., Levy, R., Bull, M., Diner, D., Martonchik, J. V., Paradise, S. R., Hansen, E. G., and Remer, L. A.: MISR Aerosol Product Attributes

and Statistical Comparisons With MODIS, IEEE T. Geosci. Remote, 47, 4095–4114, doi:10.1109/tgrs.2009.2023115, 2009.

Kahn, R., Gaitley, B. J., Garay, M. J., Diner, D. J., Eck, T. F., Smirnov, A., and Holben, B. N.: Multiangle Imaging SpectroRadiometer global aerosol product assessment by comparison with the Aerosol Robotic Network, J. Geophys. Res.-Atmos., 115, D23209, doi:10.1029/2010jd014601, 2010.

Kalashnikova, O. V., Kahn, R., Sokolik, I. N., and Li, W. H.: Ability of multiangle remote sensing observations to identify and distinguish mineral dust types: optical models and retrievals of optically thick plumes, J. Geophys. Res.-Atmos., 110, D18S14, doi:10.1029/2004jd004550, 2005.

Kaufman, Y. J., Tanre, D., Remer, L. A., Vermote, E. F., Chu, A., and Holben, B. N.: Operational remote sensing of tropospheric aerosol over land from EOS moderate resolution imaging spectroradiometer, J. Geophys. Res.-Atmos., 102, 17051–17067, doi:10.1029/96jd03988, 1997.

Lee, K. H. and Kim, Y. J.: Satellite remote sensing of Asian aerosols: a case study of clean, polluted, and Asian dust storm days, Atmos. Meas. Tech., 3, 1771–1784, doi:10.5194/amt-3-1771-2010, 2010.

Levy, R. C., Remer, L. A., Mattoo, S., Vermote, E. F., and Kaufman, Y. J.: Second-generation operational algorithm: retrieval of aerosol properties over land from inversion of Moderate Resolution Imaging Spectroradiometer spectral reflectance, J. Geophys. Res.-Atmos., 112, D13211, doi:10.1029/2006jd007811, 2007.

Li, C. C., Lau, A. K. H., Mao, J. T., and Chu, D. A.: Retrieval, validation, and application of the 1-km aerosol optical depth from MODIS measurements over Hong Kong, IEEE T. Geosci. Remote, 43, 2650–2658, doi:10.1109/tgrs.2005.856627, 2005a.

Li, Q. B., Jacob, D. J., Park, R., Wang, Y. X., Heald, C. L., Hudman, R., Yantosca, R. M., Martin, R. V., and Evans, M.: North American pollution outflow and the trapping of convectively lifted pollution by upper-level anticyclone, J. Geophys. Res.-Atmos., 110, D10301, doi:10.1029/2004jd005039, 2005b.

Li, S. S., Chen, L. F., Xiong, X. Z., Tao, J. H., Su, L., Han, D., and Liu, Y.: Retrieval of the Haze Optical Thickness in North China Plain Using MODIS Data, IEEE T. Geosci. Remote, 51, 2528–2540, doi:10.1109/tgrs.2012.2214038, 2013.

Liu, Y., Sarnat, J. A., Coull, B. A., Koutrakis, P., and Jacob, D. J.: Validation of multiangle imaging spectroradiometer (MISR) aerosol optical thickness measurements using aerosol robotic

Title Page

Abstract | Introduction

Conclusions | References

Tables | Figures

◀ | ▶

◀ | ▶

Back | Close

Full Screen / Esc

Printer-friendly Version

Interactive Discussion

network (AERONET) observations over the contiguous United States, J. Geophys. Res.-Atmos., 109, D06205, doi:10.1029/2003jd003981, 2004.

Liu, Y., Koutrakis, P., and Kahn, R.: Estimating fine particulate matter component concentrations and size distributions using satellite-retrieved fractional aerosol optical depth: Part 1 – Method development, J. Air Waste Manage., 57, 1351–1359, 2007a.

Liu, Y., Koutrakis, P., Kahn, R., Turquety, S., and Yantosca, R. M.: Estimating fine particulate matter component concentrations and size distributions using satellite-retrieved fractional aerosol optical depth: Part 2 – A case study, J. Air Waste Manage., 57, 1360–1369, 2007b.

Liu, Y., Chen, D., Kahn, R. A., and He, K. B.: Review of the applications of Multiangle Imaging SpectroRadiometer to air quality research, Sci. China Ser. D-Earth Sci., 52, 132–144, doi:10.1007/s11430-008-0149-6, 2009a.

Liu, Y., Kahn, R. A., Chaloulakou, A., and Koutrakis, P.: Analysis of the impact of the forest fires in August 2007 on air quality of Athens using multi-sensor aerosol remote sensing data, meteorology and surface observations, Atmos. Environ., 43, 3310–3318, doi:10.1016/j.atmosenv.2009.04.010, 2009b.

Lohmann, U. and Lesins, G.: Stronger constraints on the anthropogenic indirect aerosol effect, Science, 298, 1012–1015, doi:10.1126/science.1075405, 2002.

Mahowald, N.: Aerosol indirect effect on biogeochemical cycles and climate, Science, 334, 794–796, doi:10.1126/science.1207374, 2011.

Martin, R. V., Jacob, D. J., Yantosca, R. M., Chin, M., and Ginoux, P.: Global and regional decreases in tropospheric oxidants from photochemical effects of aerosols, J. Geophys. Res.-Atmos., 108, 4097, doi:10.1029/2002jd002622, 2003.

Martonchik, J. V., Diner, D. J., Kahn, R. A., Ackerman, T. P., Verstraete, M. E., Pinty, B., and Gordon, H. R.: Techniques for the retrieval of aerosol properties over land and ocean using multiangle imaging, IEEE T. Geosci. Remote, 36, 1212–1227, doi:10.1109/36.701027, 1998.

Martonchik, J. V., Diner, D. J., Kahn, R., Gaitley, B., and Holben, B. N.: Comparison of MISR and AERONET aerosol optical depths over desert sites, Geophys. Res. Lett., 31, L16102, doi:10.1029/2004gl019807, 2004.

Mian Chin, Diehl, T., Dubovik, O., Eck, T. F., Holben, B. N., Sinyuk, A., and Streets, D. G.: Light absorption by pollution, dust, and biomass burning aerosols: a global model study and evaluation with AERONET measurements, Ann. Geophys., 27, 3439–3464, doi:10.5194/angeo-27-3439-2009, 2009.

Title Page

Abstract | Introduction

Conclusions | References

Tables | Figures

◄ | ►

Back | Close

Full Screen / Esc

Printer-friendly Version

Interactive Discussion

Myhre, G.: Consistency between satellite-derived and modeled estimates of the direct aerosol effect, Science, 325, 187–190, doi:10.1126/science.1174461, 2009.

Omar, A. H., Won, J. G., Winker, D. M., Yoon, S. C., Dubovik, O., and McCormick, M. P.: Development of global aerosol models using cluster analysis of Aerosol Robotic Network (AERONET) measurements, J. Geophys. Res.-Atmos., 110, D10S14, doi:10.1029/2004jd004874, 2005.

Patadia, F., Kahn, R. A., Limbacher, J. A., Burton, S. P., Ferrare, R. A., Hostetler, C. A., and Hair, J. W.: Aerosol airmass type mapping over the Urban Mexico City region from space-based multi-angle imaging, Atmos. Chem. Phys., 13, 9525–9541, doi:10.5194/acp-13-9525-2013, 2013.

Reid, J. S., Eck, T. F., Christopher, S. A., Hobbs, P. V., and Holben, B.: Use of the Angstrom exponent to estimate the variability of optical and physical properties of aging smoke particles in Brazil, J. Geophys. Res.-Atmos., 104, 27473–27489, doi:10.1029/1999jd900833, 1999.

Russell, P. B., Bergstrom, R. W., Shinozuka, Y., Clarke, A. D., DeCarlo, P. F., Jimenez, J. L., Livingston, J. M., Redemann, J., Dubovik, O., and Strawa, A.: Absorption Angstrom Exponent in AERONET and related data as an indicator of aerosol composition, Atmos. Chem. Phys., 10, 1155–1169, doi:10.5194/acp-10-1155-2010, 2010.

Stevens, B. and Feingold, G.: Untangling aerosol effects on clouds and precipitation in a buffered system, Nature, 461, 607–613, doi:10.1038/nature08281, 2009.

van Donkelaar, A., Martin, R. V., Brauer, M., Kahn, R., Levy, R., Verduzco, C., and Villeneuve, P. J.: Global estimates of ambient fine particulate matter concentrations from satellite-based aerosol optical depth: development and application, Environ. Health Persp., 118, 847–855, doi:10.1289/ehp.0901623, 2010.

Wang, J., van den Heever, S. C., and Reid, J. S.: A conceptual model for the link between Central American biomass burning aerosols and severe weather over the south central United States, Environ. Res. Lett., 4, 015003, doi:10.1088/1748-9326/4/1/015003, 2009.

Wang, J., Xu, X. G., Spurr, R., Wang, Y. X., and Drury, E.: Improved algorithm for MODIS satellite retrievals of aerosol optical thickness over land in dusty atmosphere: implications for air quality monitoring in China, Remote Sens. Environ., 114, 2575–2583, doi:10.1016/j.rse.2010.05.034, 2010.

Wang, J., Xu, X. G., Henze, D. K., Zeng, J., Ji, Q., Tsay, S. C., and Huang, J. P.: Top-down estimate of dust emissions through integration of MODIS and MISR aerosol retrievals with the

Discussion Paper | Discussion Paper | Discussion Paper | Discussion Paper

GEOS-Chem adjoint model, Geophys. Res. Lett., 39, L08802, doi:10.1029/2012gl051136, 2012.

Yu, H. B., Remer, L. A., Chin, M., Bian, H. S., Tan, Q., Yuan, T. L., and Zhang, Y.: Aerosols from overseas rival domestic emissions over North America, Science, 337, 566–569, doi:10.1126/science.1217576, 2012.

Zhang, X. Y. and Kondragunta, S.: Temporal and spatial variability in biomass burned areas across the USA derived from the GOES fire product, Remote Sens. Environ., 112, 2886–2897, doi:10.1016/j.rse.2008.02.006, 2008.

Table 1. Validations of our work's aerosol optical properties by AERONET in different geographical regions and seasons.

		All	East	West	Spring	Summer	Fall	Winter	≤ 0.2; 0.5	> 0.2; 0.5
AOD	N	1492	570	922	401	470	390	231	1336	156
	Mean_A	0.1	0.12	0.09	0.1	0.13	0.1	0.06	0.08	0.31
	Mean_O	0.13	0.13	0.14	0.14	0.16	0.1	0.08	0.11	0.28
	Diff	0.04	0.03	0.05	0.05	0.06	0.03	0.03	0.04	0.08
	S,I	0.79, 0.04	0.81, 0.03	0.75, 0.06	0.66, 0.06	0.75, 0.04	0.8, 0.03	0.68, 0.05	0.88, 0.04	0.78, 0.03
	r	0.79	0.87	0.7	0.65	0.78	0.88	0.74	0.58	0.7
ANG	N	1492	570	922	401	470	390	231	1336	156
	Mean_A	1.27	1.39	1.19	1.06	1.36	1.4	1.21	1.23	1.55
	Mean_O	1.21	1.31	1.15	0.97	1.24	1.36	1.3	1.2	1.38
	Diff	0.32	0.31	0.33	0.28	0.32	0.33	0.38	0.32	0.31
	S,I	0.29, 0.84	0.31, 0.89	0.26, 0.84	0.3, 0.63	0.31, 0.82	0.16, 1.13	0.14, 1.15	0.26, 0.87	0.41, 0.75
	r	0.45	0.45	0.42	0.5	0.48	0.28	0.27	0.41	0.5
AAOD	N	107	81	26	14	59	31	3	79	28
	Mean_A	0.018	0.018	0.017	0.017	0.018	0.017	0.017	0.015	0.024
	Mean_O	0.013	0.012	0.017	0.0056	0.014	0.015	0.009	0.011	0.018
	Diff	0.011	0.011	0.0097	0.013	0.011	0.01	0.008	0.01	0.014
	γ	0.74	0.66	0.99	0.34	0.77	0.89	0.53	0.73	0.75
	S	0.55	0.44	0.95	0.23	0.57	0.68	0.52	0.51	0.6

Spring is Mar through May, summer is Jun through Aug, fall is Sep through Nov, and winter is Dec through Feb.
N refers to the matched AERONET and our work samples.
Mean_A and Mean_O are the mean values of AERONET and our work respectively.
Diff is calculated as the mean of absolute value of our work – AERONET.
S and I represent the slope and intercept respectively.
γ is the ratio of mean AAOD to mean AOD.

Table 2. Statistics for the mean values of MISR, GOCART and our work's aerosol optical properties over the contiguous US.

		All	East	West	Spring	Summer	Fall	Winter
AOD	MISR	0.14	0.16	0.13	0.17	0.18	0.1	0.083
	GOCART	0.092	0.11	0.079	0.12	0.1	0.075	0.058
	our work	0.14	0.15	0.13	0.17	0.18	0.097	0.082
ANG	MISR	1.24	1.34	1.16	1.15	1.19	1.32	1.34
	GOCART	1.19	1.24	1.14	0.94	1.28	1.27	1.26
	our work	1.22	1.28	1.15	1	1.26	1.32	1.31
AAOD	MISR	0.0035	0.043	0.023	0.042	0.045	0.027	0.021
	GOCART	0.0059	0.0061	0.0057	0.0081	0.006	0.0048	0.0039
	our work	0.059	0.06	0.058	0.07	0.071	0.044	0.042
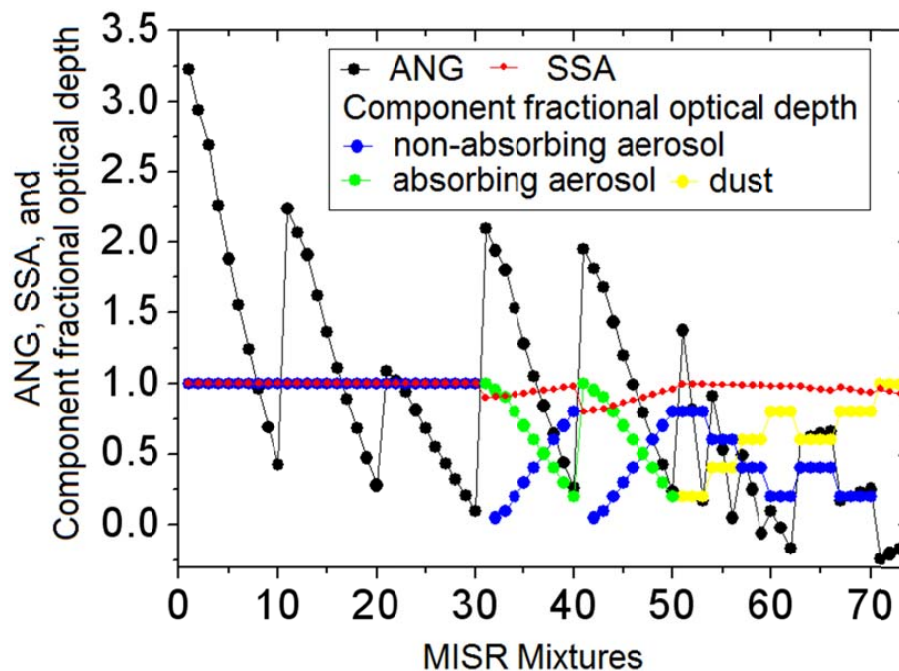
Figure 1. Distributions of Angstrom exponent, SSA at 558 nm and component fractional optical depth of MISR aerosol mixtures.

Title Page

Abstract | Introduction

Conclusions | References

Tables | Figures

|◄ | ►|

◄ | ►

Back | Close

Full Screen / Esc

Printer-friendly Version

Interactive Discussion
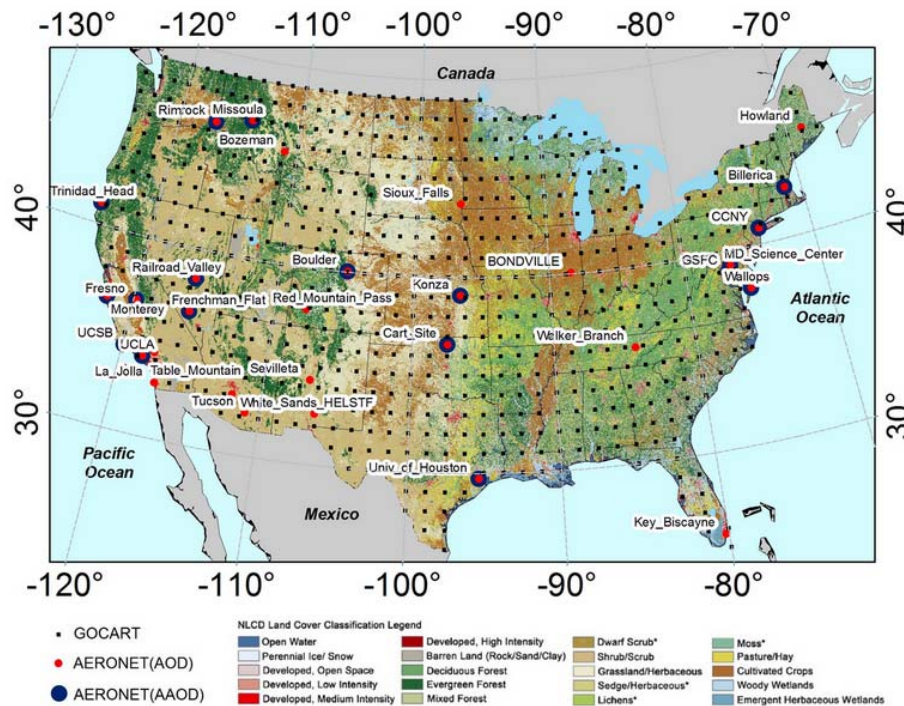
Figure 2. Spatial distribution of GOCART 1° × 1.25° (blue circles) grids in the contiguous US 32 AERONET sites containing AOD Level 2 data from 2006 to 2009 are shown as red circles. The NLCD 2006 land cover layer are created by the Multi-Resolution Land Characteristics (MRLC) Consortium (http://www.mrlc.gov/nlcd06_data.php).
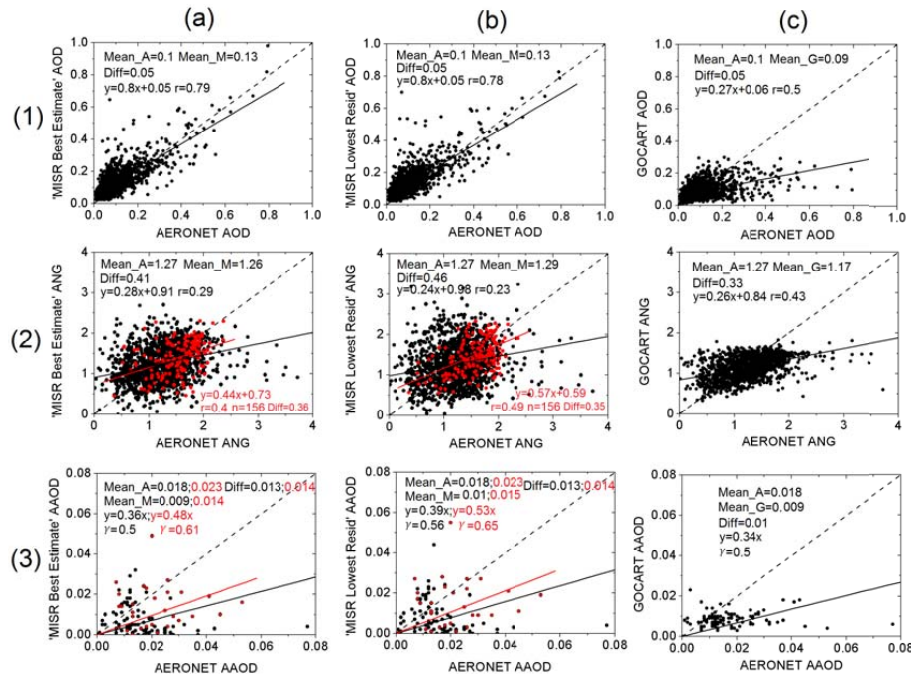
Figure 3. Validation of "MISR Best Estimate" (column a), "MISR Lowest Resid" (column b) and GOCART (column c) AOD (row 1), ANG (row 2), and AAOD (row 3) using AERONET observations. "Mean_A", "Mean_M" and "Mean_G" are the mean values of AERONET, MISR and GOCART respectively. "Diff" is calculated as the mean of absolute difference with AERONET. The dashed line represents the $y = x$ line.
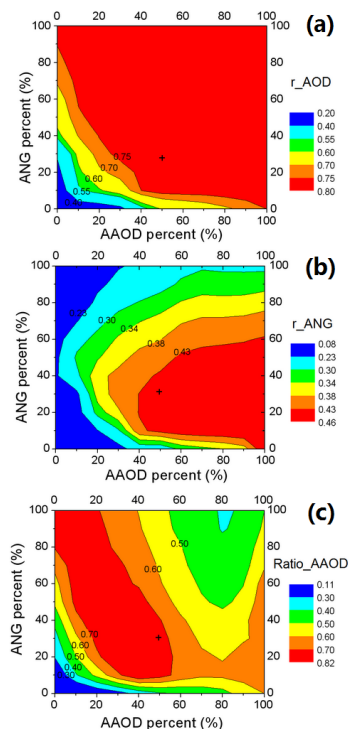
Figure 4. Sensitivity analysis for correlations between our **(a)** AOD, **(b)** ANG, **(c)** AAOD and AERONET by thresholds of ANG and AAOD. The axes specify the percent of mixtures passing the MISR retrieval acceptance criteria coming closest to the GoCART model value that is retained by our method (Eqs. 4 and 5), so a smaller number means the model is used to provide a tighter constraint. The resulting agreement is then assessed based on MISR-AERONET coincident observations.
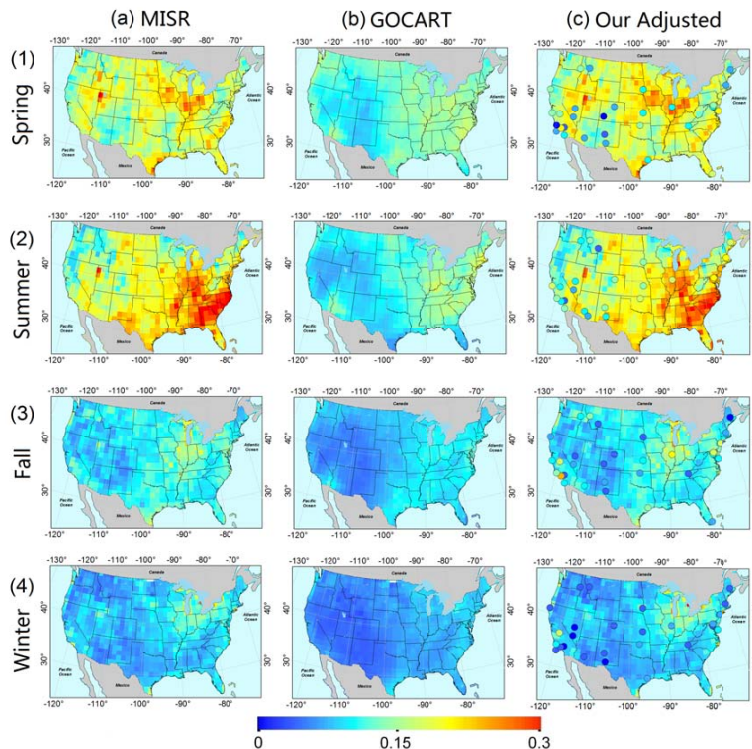
Figure 5. Distributions of seasonal averaged AOD from MISR retrievals (column a), GOCART simulations (column b), our results (column c) and AERONET measurements (superposed on our results, circles in column c) during the period of 2006 to 2009 in Spring (row 1), Summer (row 2), Fall (row 3) and Winter (row 4). AERONET and GOCART data are temporally and spatially matched with in MISR cloud free conditions.
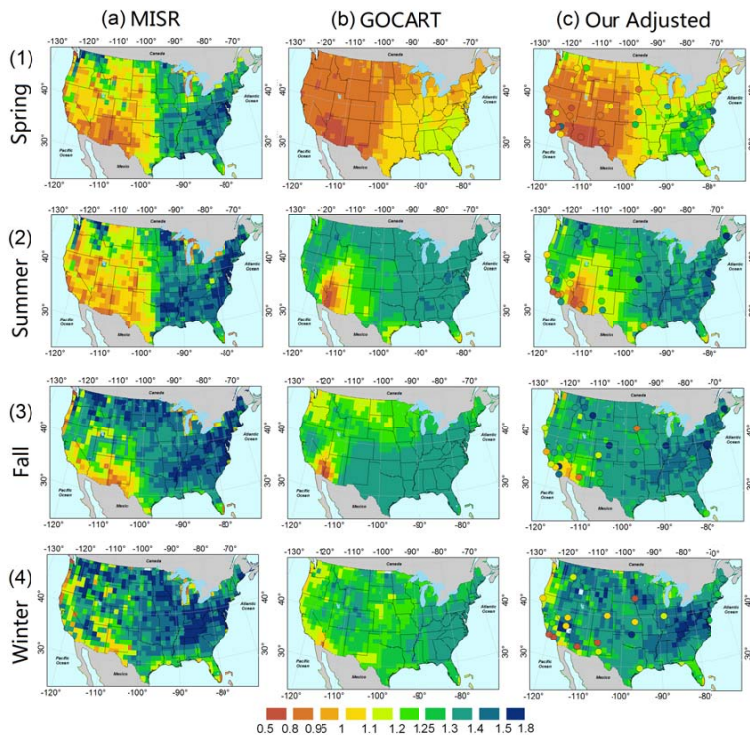
Figure 6. Same as Fig. 5 but for ANG distribution, note the color bar is from 0.5 to 1.8.

Title Page

Abstract | Introduction

Conclusions | References

Tables | Figures

|◄ | ►|

◄ | ►

Back | Close

Full Screen / Esc

Printer-friendly Version

Interactive Discussion
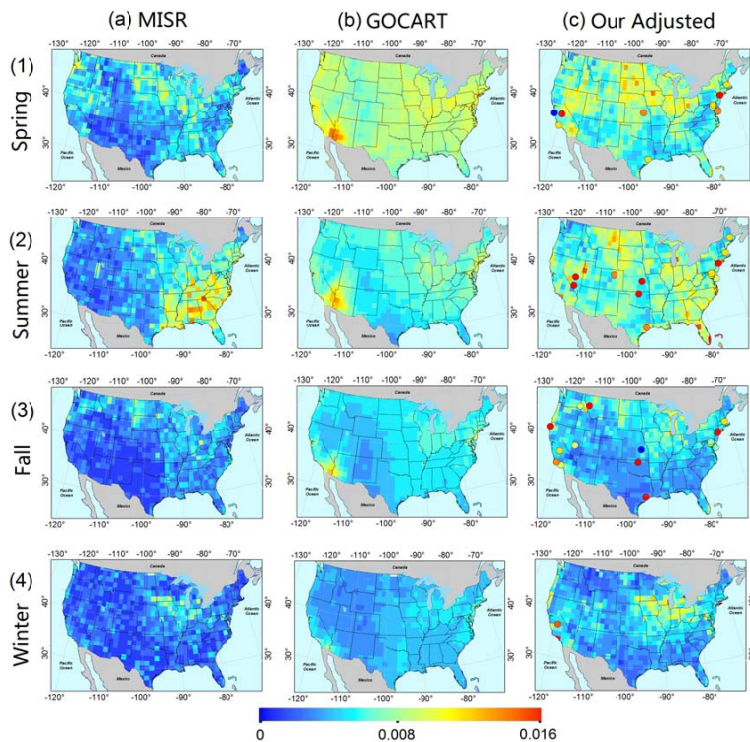
Figure 7. Same as Fig. 5 but for AAOD distribution, note the color bar is from 0 to 0.016.